

Document downloaded from:

<http://hdl.handle.net/10251/82110>

This paper must be cited as:

Meléndez-Gimeno, C.; Miguel Sosa, P.; Pallarés Rubio, L. (2016). A Simplified Approach for the Ultimate Limit State Analysis of Three-Dimensional Reinforced Concrete Elements. *Engineering Structures*. 123:330-340. doi:10.1016/j.engstruct.2016.05.039.



The final publication is available at

<https://doi.org/10.1016/j.engstruct.2016.05.039>

Copyright Elsevier

Additional Information

A Simplified Approach for the Ultimate Limit State Analysis of Three-Dimensional Reinforced Concrete Elements

Keywords:

reinforced concrete; 3D discontinuity regions; strut-and-tie method; stress fields; finite element method; pile caps; socket base column-to-foundation connections

Notation

E_{cm} secant modulus of elasticity of concrete

f_{cm} mean value of cylinder compressive strength of concrete

f_{cc} modified compressive strength of concrete

f_{cp} equivalent plastic strength of concrete

f_{ck} characteristic value of cylinder compressive strength of concrete

f_{ct} tensile strength of concrete

f_{sy} yielding strength of steel

G_{ij} tangential shear modulus

G_f fracture energy of concrete

$\varepsilon_i, \varepsilon_j, \varepsilon_k$ strain in principal directions i, j, k

ε_{cl} axial strain at unconfined concrete strength f_{cm}

ε_{cl}^* axial strain at modified concrete strength f_{cc}

$\sigma_i, \sigma_j, \sigma_k$ stress in principal directions i, j, k

1. Introduction

Computer software is widely applied in the analysis and design of reinforced concrete structures. In particular, the application of the finite element (FE) method has become most important in recent decades [1]. Although initially its use was limited mainly to the domain of researchers, today the FE method is an everyday tool in many structural design offices. The development of computing

technology and FE programmes has contributed to this spread. Guidelines and recommendations have been edited to help practitioners define the models and analyses of the results (e.g. [1][2]).

The FE method has permitted the development of advanced constitutive concrete models (e.g. [3][4][5]), which have been later implemented in FE software packages. On the one hand, the ability of some of these models to accurately reproduce the behaviour of concrete structures is doubtless. On the other hand, their complex formulation limits the number of potential users because only those who understand the fundamentals on which models are based should apply them. The calibration of model-related constants, some of which have no clear physical meaning and are difficult to understand [6][7], can also interfere with their application.

The methods that are included in concrete design codes, and have been traditionally applied in practice, adopt simplifications to deal with the complex behaviour of concrete. As stated by Schlaich et al. [8], design concepts should be clear and based on simple models that are understandable by designing engineers. The truss analogy [9][10], which became a practical and useful tool to understand the response of cracked reinforced concrete beams, is such an example. Schlaich et al. later developed the strut-and-tie method [8], which generalised the truss analogy to apply it to any part of any structure, including regions with statical and/or geometrical discontinuities (D-regions). One of its main assumptions is neglecting the tensile strength of concrete.

The stress field method [11] is also a simplified approach to design reinforced concrete structures. The tensile strength of concrete is neglected and a rigid-plastic constitutive behaviour is adopted in compression. Applications of the stress field method are similar to those of the strut-and-tie method. Strut-and-tie models can be viewed as discrete representations of stress fields. More detailed information about structural behaviour can be obtained from stress field models than from strut-and-tie models, but the former also require considerable computational effort.

Computer-based tools to balance the accuracy and adaptability of FE models, and the simplicity of design models and methods are of interest. Several computer-based tools have been developed to facilitate the use of strut-and-tie models [12][13][14] and stress field models [15][16]. These tools adopt simple concrete constitutive models, and are valuable for ultimate limit state analyses and for

designing two-dimensional D-regions. However, no references of tools that have extended the use of simple concrete models to 3D have been found.

In this paper a simplified, comprehensible 3D constitutive model for concrete is proposed and its fundamentals are described. This model characterises the 3D response of concrete by using uniaxial stress-strain laws, such as those proposed in concrete design codes, which are familiar to practitioners. Input variables are scarce and the parameters required to define the model have a clear physical meaning which allows the engineer to focus on the analysis and/or design of the structure rather than on the definition of the model. The undertaken simplifications limit the scope of the model to the ultimate limit state.

This model has been implemented into a non-linear FE-based tool developed by the authors (FESCA 3D: Finite Elements for Simplified Concrete Analysis in 3D). Two examples of applications are provided: firstly, the results obtained for 12 four-pile caps are presented and discussed. Conclusions are drawn for applying strut-and-tie models to these elements; secondly, the stress fields obtained for three socket base column-to-foundation connections demonstrate that this approach may be of interest to understand the structural behaviour of elements with complex geometries and for proposing suitable strut-and-tie models.

The proposed approach automatically allows the generation of three-dimensional stress fields from which three-dimensional strut-and-tie models can be easily developed. This feature is of interest because, for certain cases, the selection of an appropriate 3D stress field or strut-and-tie model is much more complicated than in 2D. Currently, and as addressed in fib bulletin 61 [17], there is scarce or absolutely no guidance about applying the strut-and-tie method to D-regions that display a three-dimensional behaviour. The results obtained with FESCA 3D could motivate the further study of the strut-and-tie method for 3D elements.

2. Adoption of a simplified model for concrete

2.1. On modelling concrete behaviour

Concrete is a brittle aggregate material, and its behaviour depends on its components and their interaction. Some degree of idealisation is required and justified to characterise the non-linear response of concrete structures at a macroscale level. The inherent complexity of concrete, linked

to the aspiration of accurately capturing its behaviour, has encouraged the development of various constitutive models in the last few decades. By means of different approaches, these models include diverse factors that affect concrete behaviour, such as cracking, confinement, crushing, degradation, etc. Although the accuracy of some of these models is unquestionable, their application can generally entail some difficulties for most practitioners given their complexity. Therefore, idealisation of concrete response is necessary for common engineering issues.

Some common idealisations in design codes (like in MC 2010 [18], EC 2 [19], ACI 318-14 [20]) include: (i) linear elastic behaviour, i.e. assuming uncracked cross-sections, a linear stress-strain relationship and a mean modulus of elasticity value; (ii) plastic behaviour, like the strut-and-tie method and the stress field method; and (iii) non-linear behaviour by adopting adequate non-linear behaviour for concrete. Although these models entail some loss of accuracy, it may be admissible for the sake of simplicity and safety in general practice.

The use of uniaxial stress-strain laws to characterise concrete behaviour is a common practice in the analysis and design included in plane and spatial problems. In compression, this relationship can be easily obtained from uniaxial compression tests. Standardised compressive stress-strain equations are also proposed in codes. Obtaining the stress-strain relationship in tension is also feasible, but is not as straightforward [21]. Standardised tension laws are found in the literature [22]. Notwithstanding, the lower tensile strength value of concrete compared to compressive strength, and the fact that stress drops abruptly after cracking, mean that neglecting tensile strength of concrete is common practice.

Reducing the number of parameters required to define a model is also important since it reduces the risk of making mistakes while defining them or interpreting the results, and allows engineers to focus on the analysis and/or design. In design codes, concrete compressive strength is the main parameter from which the other variables, such as modulus of elasticity or tensile strength, can be derived. The effect of transverse cracking in compression zones and confinement can be considered by modifying concrete strength.

After considering the above-mentioned issues, the authors propose a simplified, comprehensible behaviour model for concrete that adopts uniaxial stress-strain laws, such as those proposed in design codes, to characterise the response of 3D structural elements.

2.2. Model description

The adoption of an orthotropic model for concrete permits the 3D response to be split into three directions and to treat each direction separately. In this way a uniaxial stress-strain relation can be employed to model a three-dimensional phenomenon. Orthogonal models are suitable for smeared crack representations [23], where concrete is treated as a continuum, even after cracking.

As proposed by Cope et al. [24], the axes of principal strain are taken as axes of material orthotropy (Figure 1a) and coaxiality between the principal strain and principal stress directions is enforced (Figure 1b). The adoption of this model is justified for its simplicity, but some limitations must be addressed. The assumption of coaxiality is only valid when sufficient shear stress transfer takes place along the crack planes. This is not the case in high strength concrete structural elements, where cracks typically propagate through aggregates, producing smooth and flat cracks. Moreover, crack planes are not memorized and, hence, the model may provide an incorrect response for non-proportional or cyclic loadings, or when the initial cracks prior to loading are of significance [25].

For each direction, stress σ_i can be computed from its principal strain ε_i based on the adopted stress-strain curve ($F_c(\varepsilon_i)$ in compression and $F_t(\varepsilon_i)$ in tension):

$$\sigma_i = \begin{cases} F_c(\varepsilon_i) \cdot f_{cc}(\varepsilon_j, \varepsilon_k, \sigma_j, \sigma_k) & \text{if } \varepsilon_i < 0 \\ F_t(\varepsilon_i) \cdot f_{ct} & \text{if } \varepsilon_i > 0 \end{cases} \quad (1)$$

$f_{cc}(\varepsilon_j, \varepsilon_k, \sigma_j, \sigma_k)$ in Equation (1) takes into account the effect of transverse cracking and confinement on the compressive strength of concrete as follows.

Figure 1. (a) 3D orthotropic model and (b) Mohr's circle for strain and stress. Enforcing coaxiality between principal strain and stress directions

The Tension-Compression Interaction

Presence of major tensile strains that are normal to the compressive direction substantially reduces the strength and the stiffness of concrete in compression compared to the response in a standard cylinder test [26].

When transverse strains are unknown, a reduction factor can be applied, which is based on the assumed cracking pattern around the compressive flow. For the stress field and strut-and-tie models, MC 2010 [18] suggests using a factor equal: 1 for undisturbed uniaxial compression states; 0.75 if cracks are parallel to the direction of compression and if tension reinforcement is perpendicular to it; 0.55 if reinforcement runs obliquely to the direction of compression.

The reduction factor adopted in this paper is based on the Modified Compression-Field Theory (MCFT) of Vecchio et al. [26]. By testing reinforced concrete panels, the following relation for the reduction factor was obtained:

$$\frac{f_{cc}}{f_{cm}} = \frac{1}{0.8+170\varepsilon_t} \leq 1 \quad (2)$$

where ε_t is the transverse principal tensile strain.

The MCFT was later extended to 3D by Vecchio and Selby [27]. When two tensile strains appear transversely to the direction of compression, Vecchio and Selby [27] propose taking the greater tensile strain of the two, which implies neglecting the effect of the second tensile strain. The constitutive model proposed herein was developed for a computer tool that addresses engineers, where safety takes priority over precision. Hence taking ε_t in Equation (2) is suggested as the sum of the two transverse tensile strains, although this may lead to overestimate the reduction factor for certain strain states.

Compression-Compression Interaction

A Drucker-Prager yield criterion was adopted. The yield function is given by:

$$F = \sqrt{J_2} - \theta I_1 - k \quad (3)$$

where J_2 is the second deviatoric stress invariant, I_1 is the first stress invariant, and θ and k are parameters to be determined. Based on the experimental data presented in [28], the following values were considered:

$$\theta = 0.23 \quad (4)$$

$$k = 0.35 f_{cm} \quad (5)$$

At the beginning of each load/displacement step, and given the current principal stresses, the modified peak axial stress f_{cc} for each integration point derives from Equation (3).

To enforce the coaxiality between the principal strain and stress directions (i.e. $\theta_\varepsilon = \theta_\sigma$ in Figure 1b), tangential shear modulus G_{ij} should be given by the following expression proposed by Bazant [29]:

$$G_{ij} = \frac{\sigma_i - \sigma_j}{2(\varepsilon_i - \varepsilon_j)} \quad (6)$$

The above-described approach is known as the rotating smeared crack concept and permits the use of unidimensional stress-strain curves for 2D and 3D problems. This procedure has been previously implemented to analyse plane concrete elements, and provides reliable results [13][15].

2.3. Selecting uniaxial stress-strain laws

A uniaxial stress-strain relation must be defined to complete the constitutive model. Concrete responds differently in tension and in compression. The tensile strength of concrete is very low compared to its compressive strength. Moreover stress drops abruptly after reaching the maximum tensile strength. Although the compressive response depends on transverse strains, stress generally decreases gradually after reaching the peak stress. A selection of uniaxial stress-strain laws which can be used in tension and compression is described below.

Tension response

As stated earlier, neglecting the tensile strength of concrete is common practice. Indeed, this is the main assumption of the strut-and-tie method [8] and the stress field method [11], and has been implemented into some computer-based tools for 2D analyses [15][16]. However, neglecting the

tensile strength of concrete leads to predicted loads that are far below actual maximum loads when the tensile stresses between cracks are significant (the tension stiffening effect), or for structural elements with large volumes of unreinforced concrete.

Some models proposed in the literature consider tensile stresses in concrete. They generally assume a linear-elastic response for uncracked concrete and a post-peak descending branch.

The MCFT [26] considers tensile stresses in concrete and is frequently used to analyse planar reinforced concrete elements [13][30]. The relationship suggested after cracking is given by (Figure 2a):

$$F_t(\varepsilon_i) = \frac{\sigma_i}{f_{ct}} = \frac{1}{1 + \sqrt{200\varepsilon_i}} \quad (7)$$

Figure 2. Selection of a uniaxial concrete stress-strain law: (a) MCFT model (tension); (b) Hordijk's model (tension); (c) MC 2010 model, Hognestad parabola and elastic-perfectly plastic (compression).

This model was derived by testing reinforced concrete panels and was later extended to reinforced concrete solids [27]. It takes into account the tensile stresses between cracks and employs average stress-average strain relationships for cracked concrete. It relies on the tension stiffening effect, hence it is more suitable for elements with a distributed reinforcement layout. This is not always met in large structural elements, like three-dimensional D-Regions with large volumes of unreinforced concrete.

The softening model proposed by Hordijk [31] is based on the fracture mechanics theory and relates stress at crack-to-crack openings. Hordijk demonstrated that the shape of the normalised stress-crack opening relation is almost the same for most concrete types. The descending branch displays a tail in which stress gradually reaches a zero value. The equation proposed by Hordijk is (Figure 2b):

$$\frac{\sigma_i}{f_{ct}} = \left(1 + \left(c_1 \frac{w}{w_c} \right)^3 \right) e^{-c_2 \frac{w}{w_c}} - \frac{w}{w_c} (1 + c_1^3) e^{-c_2} \quad (8)$$

where w is the crack opening and w_c is the critical crack opening where the stress equals zero.

The best fit is obtained for $c_1 = 3$ and $c_2 = 6.93$. For these values, critical crack opening w_c must equal $5.14G_f / f_{ct}$, so the area under the $\sigma - w$ curve equals fracture energy G_f . The equivalent crack length concept is used to transform crack openings into crack strains, and to hence obtain $F_t(\varepsilon_i)$ in Equation (1). The equivalent length depends on the finite element volume.

These or other tensile stress-strain relations can be defined in FESCA 3D. However, some comments ought to be noted. Neglecting the tensile strength of concrete leads to clear stress field models and provides a better understanding of the resisting mechanism, which can be appealing for initial analyses and for educational purposes. However, predicted maximum loads may significantly underestimate actual maximum loads, which could lead to over-reinforced designs. The tensile stresses between cracks can be serious, but some degree of distributed reinforcement is required to permit the stress transfer between cracks, which may not be the case in elements with large volumes of concrete like 3D D-regions. Models based on the fracture mechanics theory take into account tensile stresses for small crack openings, but the stress value lowers until it reaches a zero value for a certain crack opening.

Compression response (Figure 2c)

Based on the response observed in cylindrical compressive tests, design codes propose standardised equations. For non-linear structural analyses, MC 2010 proposes the following expression:

$$F_c(\varepsilon_i) = \frac{\sigma_i}{f_{cc}} = \frac{k\eta_i - \eta_i^2}{1 + (k-2)\eta_i} \quad (9)$$

where $\eta_i = \varepsilon_i / \varepsilon_{c1}$, $k = 1.05E_{cm}|\varepsilon_{c1}| / f_{cm}$.

The Hognestad parabola adopted in the MCFT [26] is similar to this curve. Compressive stress is given by:

$$F_c(\varepsilon_i) = \frac{\sigma_i}{f_{cc}} = 2 \frac{\varepsilon_i}{\varepsilon_{c1}^*} - \left(\frac{\varepsilon_i}{\varepsilon_{c1}^*} \right)^2 \quad (10)$$

$$\varepsilon_{cl}^* = \frac{f_{cc}}{f_{cm}} \varepsilon_{cl}$$

The Theory of Plasticity can also be applied and can adopt an elastic-perfectly plastic response. For these models, Muttoni et al. [11] suggested reducing concrete strength to an effective value f_{cp} to take into account the increase in brittleness with concrete strength as:

$$\begin{aligned} f_{cp} &= f_{cm} \text{ if } f_{cm} \leq 20MPa \\ f_{cp} &= 2.7 f_{cm}^{2/3} \text{ if } f_{cm} > 20MPa \end{aligned} \quad (11)$$

Further reduction should be applied for cases in which strains of different orders of magnitude take place in the ultimate limit state.

2.4. Safety format for design

For design and checking purposes, the ultimate limit state should be verified by a partial safety factor method, in which design resistance is calculated using the design material values as input parameters for the non-linear analysis, as proposed in MC 2010. f_{cm} and f_{ct} should be substituted for their corresponding design values by dividing them by the partial safety factor for a material property γ_M . The design strength of steel can be similarly obtained. The partial factors γ_M for concrete and steel, as proposed in MC 2010 for persistent loads, are 1.5 and 1.15, respectively.

3. A brief FE model description

FESCA 3D is a non-linear FE-based tool for the analysis and design of three-dimensional concrete structural elements, which was developed by the authors. Several elements were defined to facilitate the model definition and to make its use more intuitive than other more refined FE programmes. The code was implemented into MatLab [32].

The twenty-node serendipity hexahedron was chosen for concrete modelling. To generate the hexahedral mesh, the open source platform Salome [33] was used in the pre-processing stage.

Steel reinforcement bars were introduced individually. An embedded model [34] was implemented, and allowed for considerable flexibility because the concrete mesh can be completely independent of the steel layout.

Defining the support and load conditions

Defining the proper boundary conditions is always important for the structural analysis. Results can vary if the local constraints at the supports or loads are not properly defined, especially for elements whose support/load dimensions are large compared to the global dimensions of the element. It is sometimes necessary to include the supports or the element that transfer(s) the load explicitly in the model, which implies more FE and additional work.

Bearings can be modelled explicitly or implicitly in FESCA 3D, and the latter simplifies the modelling process. Apart from the classic displacement constraint, a constant stress distribution support condition was implemented. It automatically generates a uniform stress field in the defined support area in one, two or three local direction(s). This is achieved by accordingly introducing a supplementary stiffness matrix into the global stiffness system. This supplementary matrix is computed internally by the programme, which entails that the load carried by each node located inside the bearing area is proportional to its tributary area, thus conferring constant stress distribution.

Regarding load modelling, it is usually assumed that loading results in a constant stress distribution under the loading plate. FESCA 3D also allows the implicit consideration of the effect of the loading plate/column stiffness in the stress distribution. It computes a stiffness matrix, based internally on the geometry and modulus of elasticity of the plate/column input by the user, which is introduced accordingly into the global stiffness system.

4. Examples of applications

4.1. Analysis, results and discussion of twelve four-pile caps

Pile caps are structural elements used to transfer a load from a column to a group of piles, and are very common in construction [35]. For their design, two types of methods are proposed in concrete codes: sectional approaches and strut-and-tie models. The use of sectional approaches for pile cap design can prove inadequate because pile caps are three-dimensional D-regions with complex non-linear strain distributions which are not considered in these methods [35][36]. The use of strut-and-tie models has proven a more rational approach, and has also provided a clear understanding of physical behaviour [35][36][37][38].

Based on a standard four-pile cap strut-and-tie model, Souza et al. [35] proposed the following equation to obtain the maximum column load resisted by a four-pile cap:

$$N_f \leq \begin{cases} N_{ff} = \frac{4A_{SD}f_{sy}d\phi_f}{e} \rightarrow \text{flexure failure mode} \\ N_{fs} = 2.08bdf_c^{2/3} \rightarrow \text{shear failure mode} \end{cases} \quad (12)$$

where A_{SD} is the total amount of bunched and grid reinforcement in one direction, d is the effective depth of the pile cap, e is the distance between the centre of piles and b represents the column dimensions.

In this formulation, shear failure is assumed to be related to the splitting of compressive struts. The flexure failure load is obtained directly from the geometry of a standard four-pile cap strut-and-tie model. Coefficient ϕ_f is included to calibrate the model based on experimental test data, and obtains a value of ϕ_f that equals 2.05. Notwithstanding, this parameter offers no physical reasoning, which implies that some uncertainties still exist, especially in relation to finding the position of the nodal zone underneath the column and the real effective depth [39]. A physical explanation for calibration factor ϕ_f should be found.

This section provides the results obtained with FESCA 3D for the analysis of the six four-pile cap models tested by Suzuki et al. [40]. These specimens were considered in [35] to calibrate ϕ_f . The purpose was to enlighten readers as to the response of pile caps and the application of strut-and-tie models for the analysis and design of these elements.

Description of specimens

The six four-pile cap models are classified according to a reinforcement arrangement (BP stands for uniform grid and BPC for a bunched square arrangement over piles), pile depth (20 cm or 30 cm) and the side length of the square column (25 cm or 30 cm). The other dimensions are identical: slab square plane 80 cm, pile diameter 15 cm, a distance between pile centres of 50 cm and column height 20 cm. In the experimental programme, two specimens per model were prepared.

The concrete cylindrical uniaxial strengths and the number of reinforcing rebars in each direction are provided in Table 1. The yield and ultimate stress for steel was 405 MPa and 592 MPa, respectively.

In Table 1, B, S and BS respectively stand for flexural failure, corner shear failure and shear failure preceded by bending yield according to [40]. Corner shear failure refers to thrusting of one or two pile bearings into the slabs. Since reinforcement strains were not measured, bending yield is defined at the point at which the deflection begins to grow quickly without a rapid decrease in load. As shown in Table 1, the authors suggested that the maximum load was preceded by an apparent bending yielding of reinforcement in all the specimens, except in BP-30-30-1 and BP-30-25-2.

*Table 1. Summary of the four-pile caps tested by Suzuki et al. [39]. *B: Flexural failure. S: Corner shear failure*

The FE Analysis

A regular FE mesh of 1014 (13x13x6) twenty-node hexahedrons was used for the 12 specimens. Only the cap itself was modelled. The supports were defined at the pile locations by employing the constant stress distribution support condition. The horizontal resistance at the supports was dismissed. The load was applied to the top of the cap and column stiffness was considered implicitly by using the option detailed in section 3.

To address the importance of the adopted constitutive model of concrete in tension, three different tensile stress-strain equations were employed: (i) neglecting the tensile strength of concrete; (ii) the MCFT law and (iii) Hordijk's model.

In the MCFT and Hordijk's model, f_{ct} was taken to equal the lower bound value of the characteristic tensile strength of concrete, as defined in MC 2010 ($f_{ct} = 0.21f_{ck}^{2/3}$). The fracture energy for Hordijk's model was also taken from the formula proposed in MC 2010 ($G_f = 73f_{cm}^{0.18}$).

To study the influence of the stress-strain relation in compression, an elastic-perfectly plastic and a parabolic law were employed. In the former, the considered modulus of elasticity equalled

$$E = 21.5 \left(\frac{f_{cm}}{10} \right)^{1/3},$$
 as proposed in MC 2010. In the latter, a value of -0.002 was adopted for ε_{cl} .

Results and discussion

The predicted maximum loads P_{FE} for the 12 specimens, by adopting the above-mentioned uniaxial stress-strain laws, are provided in Table 2. The failure loads obtained according to Equation (15) [35] were also calculated. From these results, the average μ and the coefficient of variation CV of their corresponding safety factors ($SF = P_{\max,exp} / P_{FE}$) were calculated.

Table 2. Predicted ultimate loads and the average μ and coefficient of variation CV of their corresponding safety factors SF. Notation: (i) neglecting concrete tensile strength; (ii) adopting the MCFT model; and (iii) adopting Hordijk's model.

In every finite element analysis case, the maximum load was preceded by several or all the steel rebars being yielded.

For the twelve specimens, similar results were obtained when adopting compression in an elastic-perfectly plastic or a parabolic model. Failure in specimens with low quantities of steel, such as those presented herein, is often governed by yielding reinforcement, and the concrete response in compression slightly affects the maximum load.

The obtained predicted maximum loads indicated that concrete tensile stresses play an important role in the response of pile caps. When the tensile strength of concrete was neglected, the predicted maximum loads were below the experimental values (average safety factor of 1.20-1.23). Underestimation was higher for grid reinforcement (BP) than for bunched reinforcement (BPC). This is a reasonable result because the tension stiffening effect is more significant in the former elements.

Neglecting the tensile strength of concrete is actually the main assumption of the strut-and-tie method, which in the model proposed by Souza et al.[35], justifies that the flexure failure load obtained from a theoretical four-pile cap strut-and-tie model needs to be increased by a calibration

factor in order to approach the actual experimental maximum load. The value ϕ_f obtained by Souza et al. doubled the theoretical load obtained from the strut-and-tie model, while the FE model that neglected the tensile strength of concrete underestimated the maximum load by a factor of 1.20-1.23. This difference was explained by the resulting strut angles in the models. In the model proposed by Souza et al., the idealised diagonal struts went from the centre of the column to the centre of the piles. In the FE model, the angles of the compressive stresses were steeper because the geometry of the piles and the column were considered. Therefore, the ties for the same vertical force were demanded less in the FE model than in the strut-and-tie model (see Figure 3).

The average safety factor for the 12 specimens obtained by the adaptable strut-and-tie model by Souza after applying calibration parameter ϕ_f came closer to 1 than the average safety factor when applying the FE model and neglecting the tensile strength of concrete (1.03 vs. 1.20). However, the variation of the results was wider (coefficient of variation 0.14 vs. 0.07). The FE model considered more factors than the strut-and-tie model (e.g., pile dimensions, column dimensions, the stress state underneath the column) and allowed a better pile cap response, which is an improvement over the strut-and-tie model.

Figure 3. Strut-and-tie model vs. FE model. (a) A standard three-dimensional strut-and-tie model for four-pile cap; (b) an FE model plot of concrete principal compressive stress directions for pile cap model BPC-30-30 after neglecting the tensile strength of concrete; (c) projection view of (a) on the diagonal plane; (d) projection view of (b) on the diagonal plane.

Notwithstanding, considering the tensile strength of concrete appears necessary to obtain more accurate maximum loads. For example, the strut-and-tie-based method proposed in [36] considered the contribution of the tension stiffening effect to evaluate the strength of the steel ties as follows:

$$F_{ct} = 0.2\sqrt{f_{cm}}A_{ct}$$

$$A_{ct} = \frac{d}{4} \left(\frac{l_e}{2} + \frac{d_p}{2} \right)$$

where d is the effective depth, l_e is pile spacing and d_p is the pile diameter.

Regarding the finite element model results, when considering the tension stiffening effect by adopting the MCFT, the maximum loads for the 12 specimens were overestimated (average safety factor of 0.82-0.83). The tensile stress-tensile strain relation proposed by the MCFT accounts for the concrete tensile stresses between cracks. However, the pile caps treated in this section, and generally in most 3D D-regions, obtained large volumes of unreinforced concrete, and it was not possible to guarantee the tension stiffening effect throughout the element.

The best predictions were obtained when adopting the softening law proposed by Hordijk. This model can be considered an intermediate approach between fully neglecting the tensile strength of concrete and relying excessively on the tension stiffening effect as in the MCFT: tensile stresses are admissible, but they gradually reach a zero value for relatively large strains. The average value of the safety factor came very close to 1 (1.01) and presented a small coefficient of variation (0.03-0.04).

The failure modes identified in the numerical analysis adopting Hordijk's model are included in Table 2. Apart from specimen BP-30-25-2, all specimen failures are labelled as shear failure preceded by bending yield. For specimen BP-30-25-2, the maximum load is reached with some steel rebars yielding, but the load-displacement does not show an inflection previous to the maximum load which could point to a bending yield. Indeed, if rebar yielding areas are identified it can be seen that the propagation of the yielding for this specimen is much more limited than in the other specimens. In general the identified failure modes agree with the experimental observations reported in [40]. Regarding specimens BPC-20-30-1 and BPC-20-30-2, the difference observed between experimental and numerical observations could be explained as steel hardening after yielding, which is significant for the used rebars, has been neglected in the model.

The size effect on the shear strength of pile caps is of importance and is included in some design codes. Based on the obtained safety factors, it can be said that for the specimens treated when the Hordijk's model is used the proposed model captures this effect.

When taking the results obtained from Hordijk's model as reference, the contribution of the tensile stresses to the strength of the ties at the loads near the maximum load was negligible because the

maximum load in each analysis case was achieved after yielding all or some of the reinforcement bars, which implies substantial tensile strains. The observed increment of the maximum load was due to the effect of the tensile stresses on the compressive stress flow, which led to steeper compressive stress angles at the meeting areas with reinforcement over piles (Figure 4). So based on these results, although the tensile stresses in concrete contributed to pile cap strength, their effect should not be understood as a strengthening of steel ties, as proposed in [36].

Figure 4. FE model plot of the concrete principal compressive stress directions for pile cap model BPC-30-30 by adopting Hordijk's softening law ($P=900kN$). (a) 3D view, (b) plan view and (c) projection view on the diagonal plane.

The results obtained in the FE model can provide a rational explanation for calibration coefficient ϕ_f used in the strut-and-tie model as proposed in [35]. This factor implicitly considers the effect of tensile stresses, the dimensions of piles and the column, and the stress state underneath the column. As explained above, all these factors affect the compressive stress flow, which means that the angles formed between the compressive stresses and the reinforcement rebars were steeper than assumed in the strut-and-tie model, hence the maximum load obtained for flexure failure needs to be increased. Yet when constant factor ϕ_f was applied regardless of the pile and column dimensions or the concrete tensile strength, it led to predictions with a relatively high coefficient of variation.

4.2. Analyses and results of three socket base column-to-foundation connections

A socket base column-to-foundation connection consists in a foundation element with a cavity in its upper part in which a precast column is embedded. Although its use in precast concrete structures is common, very little research has focused on them [41]. In this section the three column-foundation connections tested by Gutiérrez [42] were analysed with FESCA 3D.

Description of specimens

The experimental programme conducted by Gutiérrez focused on the three-dimensional behaviour of the foundation element. Its dimensions were 1.4m x 1.4m x 1.0m (xyz). The cavity where the column was embedded measured 0.6m x 0.5m x 0.6m (xyz). A reusable steel column was employed

to apply the load. By applying an eccentric load to the column, two horizontal loads on the vertical walls of the hole and one vertical load at the base of cavity were transferred to the foundation element. Eight load cells were used to measure the load applied inside the cavity by the column.

Firstly, and in order to design the reinforcement, Gutiérrez proposed three base strut-and-tie models. From them, ten different reinforcement configurations were established, which yielded 10 specimens to be tested. Specimens X2, X3 and X7 were considered in this section (Figure 5). The reinforcement layout of these specimens corresponded to the three base strut-and-tie models. Reinforcement in the other specimens was obtained as a combination of these three base layouts. The cylindrical uniaxial strengths of concrete for specimens X2, X3 and X7 were 28.0 MPa, 27.4 MPa and 43.1 MPa, respectively. The yield stress for steel was 530 MPa. Rebar diameters were 8, 12, 16 or 20 mm.

Figure 5. Reinforcement layout. (a) Specimen X2, (b) Specimen X3 and (c) Specimen X7.

The FE Analysis

An FE mesh of 1875 twenty-node hexahedrons was used for the three specimens. The reinforcement bars were introduced individually. The relation between the loads applied by the column inside the cavity depended on element stiffness, and varied slightly during the experimental test. To simplify the numerical analysis, it was assumed that this relation was constant for each specimen and equalled the relation observed in the test when the maximum upper horizontal load was reached. The upper horizontal load was considered to compare the experimental and numerical results.

The main purpose of this section was to show the capacity of the proposed simplified approach to facilitate the identification of the flow of forces, and to indicate the proposal of 3D strut-and-tie model for structural elements with complex geometries. Therefore, only the results obtained by neglecting the tensile strength of concrete are presented.

Results

The maximum experimental values of the upper horizontal load for specimens X2, X3 and X7 were 869kN, 762kN and 924kN, respectively. The corresponding predicted values obtained with FESCA

3D when neglecting the tensile strength of concrete were 811kN, 810kN and 878kN. In specimens X2 and X7, the predicted maximum load was limited by yielding the horizontal stirrups around the cavity. In specimen X3 the predicted maximum load was limited by yielding the horizontal rebars under the cavity in the longitudinal direction and the vertical rebars at the front wall. These failure modes agree with the experimental observations.

Thus far the proposal of strut-and-tie models for elements with complex geometries, such as the socket base column-to-foundation connections treated herein, was not straightforward. In addition, understanding the structural behaviour of these elements is not easy task. The solution achieved herein by plotting the compressive stress directions obtained in the FE model helps overcome these difficulties and enlightens the understanding of the physical behaviour of these elements (Figures 6 and 7).

Figure 6. The FE model plot of the concrete principal compressive stress directions for specimen X2 (FH=700kN) (left) and the proposed strut-and-tie model (right).

Figure 7. The FE model plot of the concrete principal compressive stress directions for specimen (a) X3 and (b) X7 (FH=700kN) (left) and the proposed strut-and-tie models (right).

5. Conclusions

This paper describes the adoption of a simplified comprehensible constitutive model for the analysis of 3D reinforced concrete structural elements. The use of complex models, like those available in the literature, can entail some difficulties for most practitioners, which should be applied only by those who understand the fundamentals on which they are based. Alternatively, the simplified approach proposed herein idealises concrete behaviour by allowing the use of uniaxial stress-strain relationships, which are familiar to engineers, in order to characterise the 3D response.

This constitutive model was implemented into the non-linear finite element-based tool FESCA 3D, which was developed by the authors to analyse three-dimensional concrete structural elements. The aim was to combine the accuracy and adaptability of FE models and the simplicity of the

proposed concrete constitutive model in order to provide an alternative tool to more refined complex finite element software packages.

If the tensile strength of concrete is neglected in the model, the simplified approach proposed herein can be used to study the kindness of the strut-and-tie method and the stress field method to analyse structural elements that display a three-dimensional behaviour. These methods are rational analysis and design tools that replace empirical approaches and rules of thumb. Notwithstanding, guidelines to apply 3D strut-and-tie models and 3D stress field models are scarce.

The application of this simplified analysis approach was shown by means of two examples: firstly, the proposed model was used in the analysis of 12 four-pile caps. The predicted maximum loads, obtained by adopting different concrete stress-strain laws, were compared, and the influence of the tensile strength of concrete was discussed. The best predictions were made the tensile strength of concrete was considered and by adopting Hordijk's model for tension softening. When the tensile strength of concrete was neglected, the effect of tensile stresses on the compressive flow was dismissed, which led to lighter maximum loads when failure was limited by steel yielding. Nevertheless, this decrease in accuracy is acceptable for design purposes. Analogously, the use of strut-and-tie models for pile caps also underestimated maximum loads. This underestimation can become even greater if the geometry of the piles and the column is not considered; secondly, the applicability of the model to generate three-dimensional stress field models for structural elements with complex geometries was proven by modelling three socket base column-to-foundation connections. Being able to view the principal compressive directions facilitates the identification of flow of forces and the development of 3D strut-and-tie models, and provides a better understanding of the structural response.

Acknowledgements

The authors wish to thank the Spanish Ministry of Education for the FPU fellowship FPU12-01459 received by the first author, and the Spanish Ministry of Economy and Competitiveness for funding Project BIA 2012-32300.

References

- [1] FIB bulletin 45. Practitioners' guide to finite element modelling of reinforced concrete structures. 2008.
- [2] Dutch Ministry of Infrastructure and Environment. Guidelines for Nonlinear Finite Element Analysis of Concrete Structures. 2012.
- [3] Bažant ZP, Oh BH. Microplane Model for Progressive Fracture of Concrete and Rock. *J Eng Mech* 1985;111:559–82. doi:10.1061/(ASCE)0733-9399(1985)111:4(559).
- [4] Hauke B, Maekawa K. Three-dimensional R/C-model with multi-directional cracking. *Comput. Model. Concr. Struct.*, 1998, p. 93–102.
- [5] Grassl P, Jirásek M. Damage-plastic model for concrete failure. *Int J Solids Struct* 2006;43:7166–96. doi:10.1016/j.ijsolstr.2006.06.032.
- [6] Kučerová A, Lepš M. Soft computing-based calibration of microplane M4 model parameters: Methodology and validation. *Adv Eng Softw* 2014;72:226–35. doi:10.1016/j.advengsoft.2014.01.013.
- [7] Jiang H, Zhao J. Calibration of the continuous surface cap model for concrete. *Finite Elem Anal Des* 2015;97:1–19. doi:10.1016/j.finel.2014.12.002.
- [8] Schlaich J, Schafer K, Jennewein M. Toward a Consistent Design of Structural Concrete. *PCI J* 1987:74–92.
- [9] Ritter W. Die Bauweise Hennebique. *Schweizerische Bauzeitung* 1899;17:41–3,49–52,59–61.
- [10] Mörsch E. Reinforced Concrete Construction, Theory and Application (Der Eisenbetonbau, seine Theorie und Anwendung). 1908.
- [11] Muttoni A, Schwartz J, Thürlimann B. Design of concrete structures with stress fields. Birkhäuser Verlag; 1997.
- [12] Tjhin TN, Kuchma DA. Integrated analysis and design tool for the strut-and-tie method. *Eng Struct* 2007;29:3042–52. doi:10.1016/j.engstruct.2007.01.032.
- [13] Park J, Yindeesuk S, Tjhin T, Kuchma D. Automated Finite-Element-Based Validation of Structures Designed by the Strut-and-Tie Method. *J Struct Eng* 2010;136:203–10.
- [14] Bairán García JM. Generación automática de esquemas de bielas y tirantes considerando criterios constructivos. *Hormigón y acero* 2012;63:67–79.
- [15] Fernández Ruiz M, Muttoni A. On Development of Suitable Stress Fields for Structural Concrete. *ACI Struct J* 2007;104:495–502.
- [16] Lourenço MS, Almeida JF. Adaptive Stress Field Models : Formulation and Validation. *ACI Struct J* 2013;110:71–81.

- [17] Reineck K, Lourenço MS, Almeida JF, Haugerud S. Gaining Experience with Strut and Tie Models for the Design of Concrete Structures. Des. Examples Strut-and-Tie Model. fib Bull. 61, 2011, p. 197–216.
- [18] Fédération Internationale du Béton. Model Code 2010. Lausanne: 2013.
- [19] European Committee for Standardization. Eurocode 2: Design of Concrete Structures - Part 1-1: General rules and rules for buildings. 2004.
- [20] ACI Committee 318. ACI 318-14: Building Code Requirements for Structural Concrete and Commentary. 2014.
- [21] Van Mier JG., van Vliet MR. Uniaxial tension test for the determination of fracture parameters of concrete: state of the art. Eng Fract Mech 2002;69:235–47. doi:10.1016/S0013-7944(01)00087-X.
- [22] Reinhardt HW, Cornelissen HAW, Hordijk DA. Tensile Tests and Failure Analysis of Concrete. J Struct Eng 1986;112:2462–77.
- [23] Rashid YR. Ultimate strength analysis of prestressed concrete pressure vessels. Nucl Eng Des 1968;7:334–44. doi:10.1016/0029-5493(68)90066-6.
- [24] Cope RJ, Rao PV, Clark LA, Norris P. Modelling of Reinforced Concrete Behaviour for Finite Element Analysis of Bridge Slabs. Numer. Methods Nonlinear Probl. 1, 1980, p. 457–70.
- [25] Boonpichetvong M, Rots JG. Fracture Analyses of Walls Under Non-Proportional Loadings. Fract. Mech. Concr. Concr. Struct., 2005, p. 8.
- [26] Vecchio FJ, Collins MP. The Modified Compression-Field Theory for Reinforced Concrete Elements Subjected to Shear. ACI J Proc 1986;83:219–31. doi:10.14359/10416.
- [27] Vecchio FJ, Selby RG. Toward Compression-Field Analysis of Reinforced Concrete Solids. J Struct Eng 1991;117:1740–58.
- [28] Hannant DJ. Nomograms for the failure of plain concrete axial stresses. Struct Eng 1974;52:151–65.
- [29] Bazant ZP. Comment on Orthotropic Models for Concrete and Geomaterials. J Eng Mech 1983;109:849–65.
- [30] Amini Najafian H, Vollum RL. Design of planar reinforced concrete D regions with nonlinear finite element analysis. Eng Struct 2013;51:211–25. doi:10.1016/j.engstruct.2013.01.022.
- [31] Hordijk D. Local approach to fatigue of concrete. Delft University of Technology, 1991.
- [32] MATLAB. version 8.4.0 (R2014b). Natick, Massachusetts: The MathWorks Inc.; 2014.
- [33] CEA/DEN, EDF R&D OC. Salome: The Open Source Integration Platform for Numerical Simulation n.d.
- [34] Elwi AE, Hrudey TM. Finite Element Model for Curved Embedded Reinforcement. J Eng Mech 1989;115:740–54. doi:10.1061/(ASCE)0733-9399(1989)115:4(740).

- [35] Souza R, Kuchma D, Park J, Bittencourt T. Adaptable Strut-and-Tie Model for Design and Verification of Four-Pile Caps. *ACI Struct J* 2009;106:142–50.
- [36] Park J, Kuchma D, Souza R. Strength predictions of pile caps by a strut-and-tie model approach. *Can J Civ Eng* 2008;35:1399–413.
- [37] Adebar P, Kuchma D, Collins MP. Strut-and-Tie Models for the Design of Pile Caps: An Experimental Study. *ACI Struct J* 1990;87:81–92.
- [38] Siao W Bin. Strut-and-Tie Model for Shear Behavior in Deep Beams and Pile Caps Failing in Diagonal Splitting. *ACI Struct J* 1993;90:356–63.
- [39] Windisch A. Discussion of Adaptable Strut-and-Tie Model for Design and Verification of Four-Pile Caps. *ACI Struct J* 2010:119–20.
- [40] Suzuki K, Otsuki K, Tsubata T. Influence of Bar Arrangement on Ultimate Strength of Four-Pile Caps. *Trans Japan Concr Inst* 1998;20:195–202.
- [41] Canha RMF, Jaguaribe K de B, El Debs ALH de C, El Debs MK. Analysis of the behavior of transverse walls of socket base connections. *Eng Struct* 2009;31:788–98. doi:10.1016/j.engstruct.2008.11.008.
- [42] Gutiérrez Vela M. Estudio Experimental de Cálices de Hormigón Armado Mediante Modelos de Bielas y Tirantes Tridimensionales (MSc Thesis). Universitat Politècnica de Valencia, 2015.

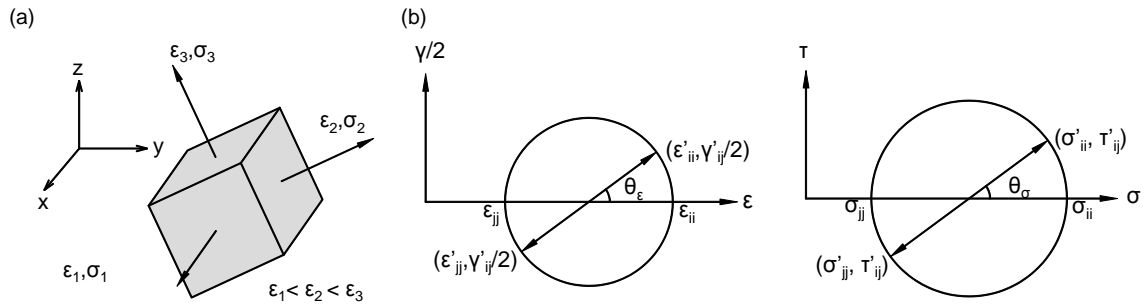


Figure 1. (a) 3D orthotropic model and (b) Mohr's circle for strain and stress. Enforcing coaxiality between principal strain and stress directions

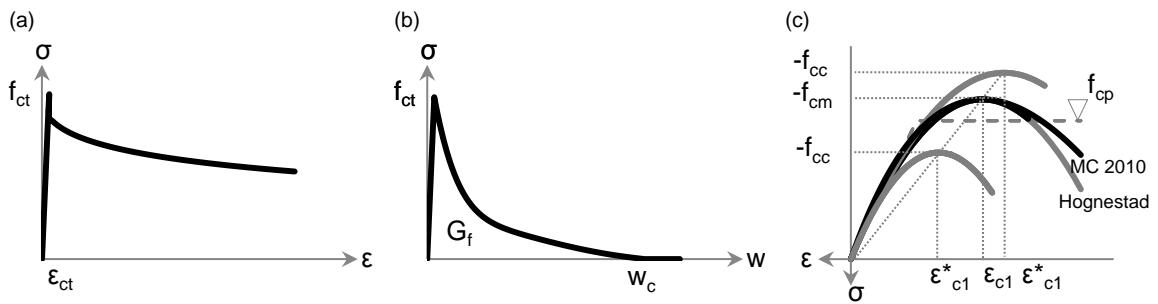


Figure 2. Selection of a uniaxial concrete stress-strain law: (a) MCFT model (tension); (b) Hordijk's model (tension); (c) MC 2010 model, Hognestad parabola and elastic-perfectly plastic (compression).

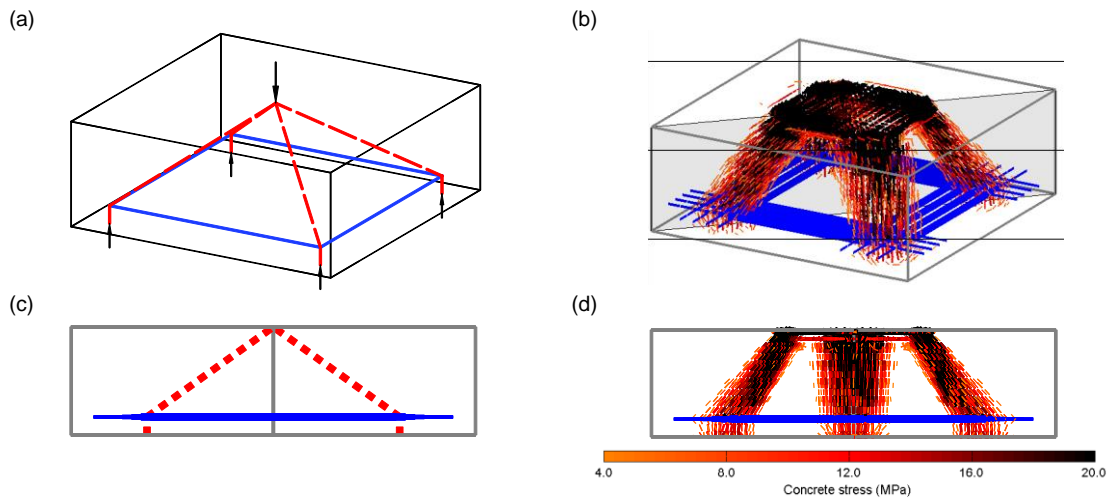


Figure 3. Strut-and-tie model vs. FE model. (a) A standard three-dimensional strut-and-tie model for four-pile cap; (b) an FE model plot of concrete principal compressive stress directions for pile cap model BPC-30-30 after neglecting the tensile strength of concrete; (c) projection view of (a) on the diagonal plane; (d) projection view of (b) on the diagonal plane.

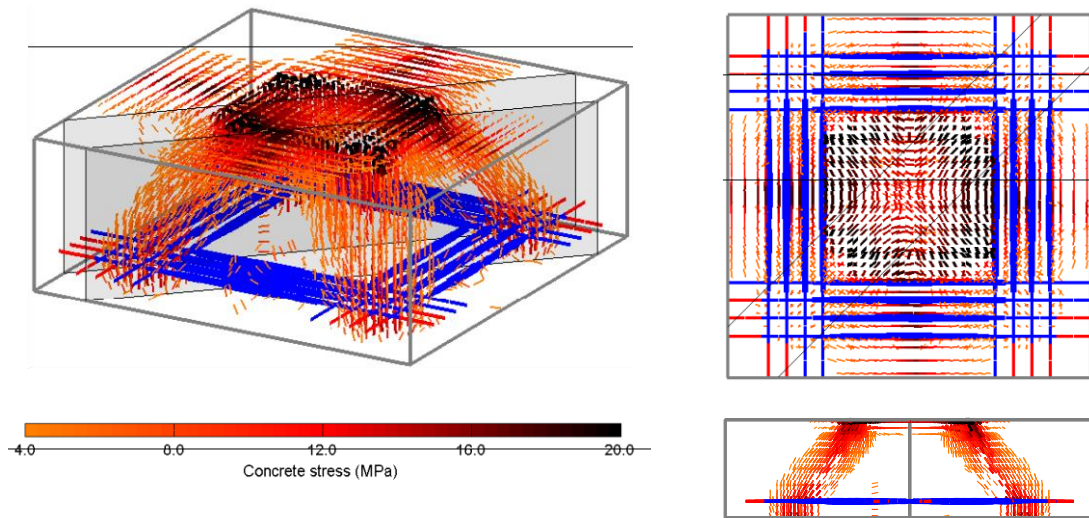


Figure 4. FE model plot of the concrete principal compressive stress directions for pile cap model BPC-30-30 by adopting Hordijk's softening law ($P=900\text{kN}$). (a) 3D view, (b) plan view and (c) projection view on the diagonal plane.

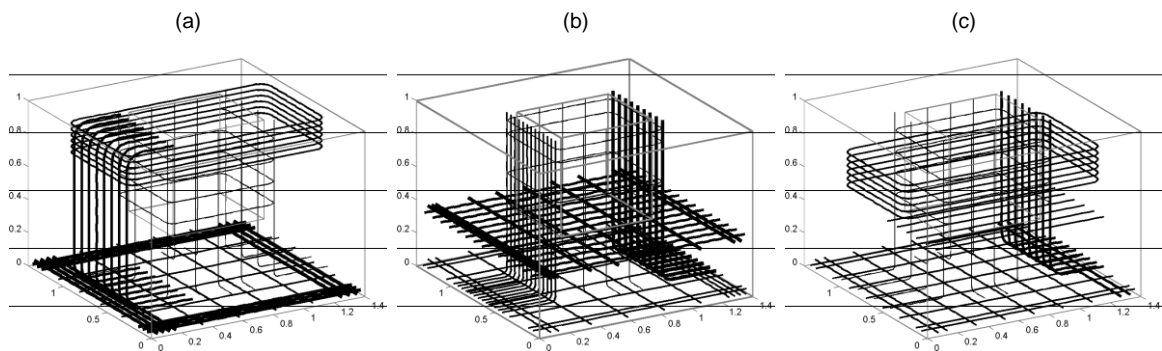


Figure 5. Reinforcement layout. (a) Specimen X2, (b) Specimen X3 and (c) Specimen X7.

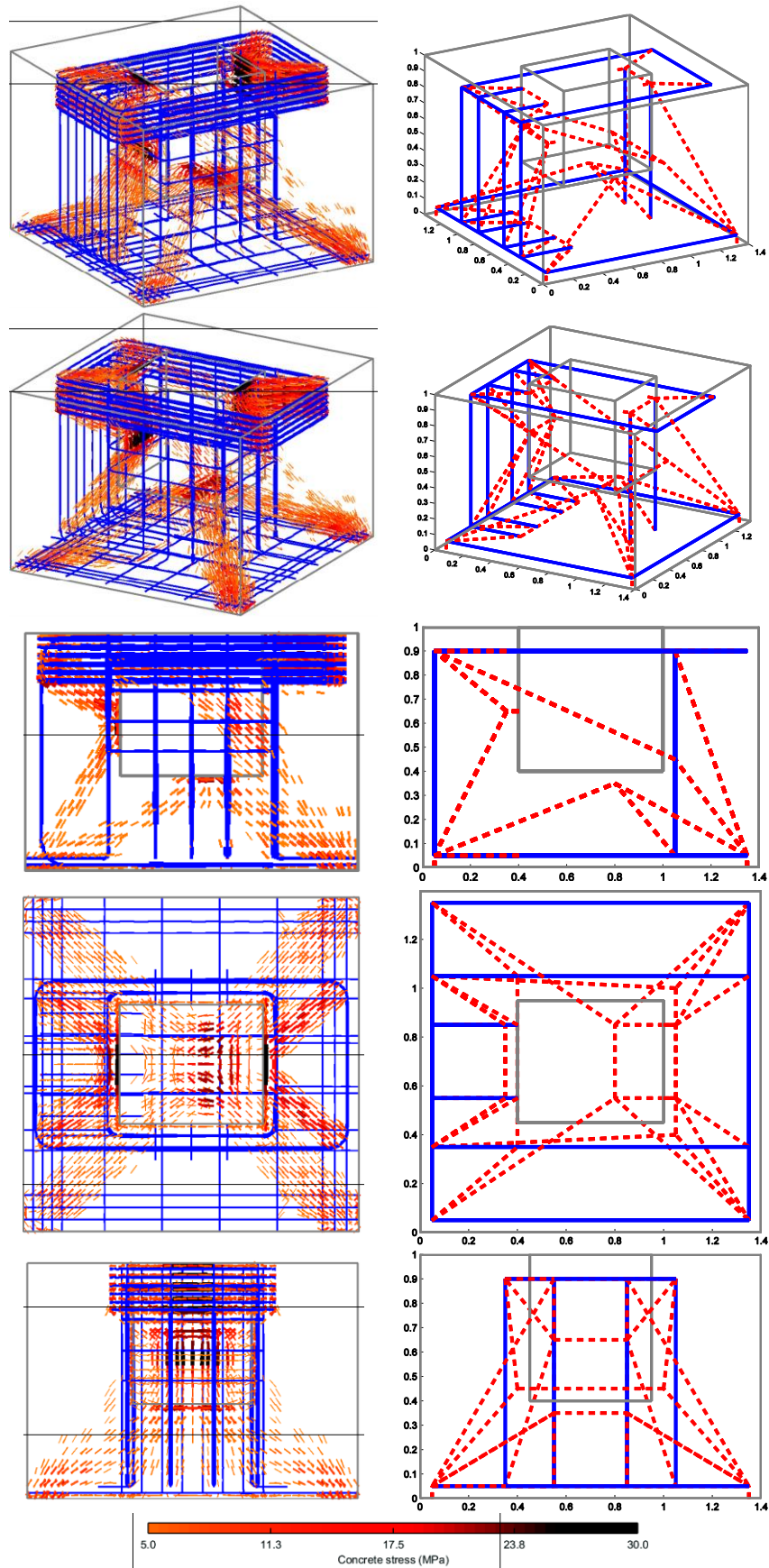


Figure 6. The FE model plot of the concrete principal compressive stress directions for specimen X2 (FH=700kN) (left) and the proposed strut-and-tie model (right).

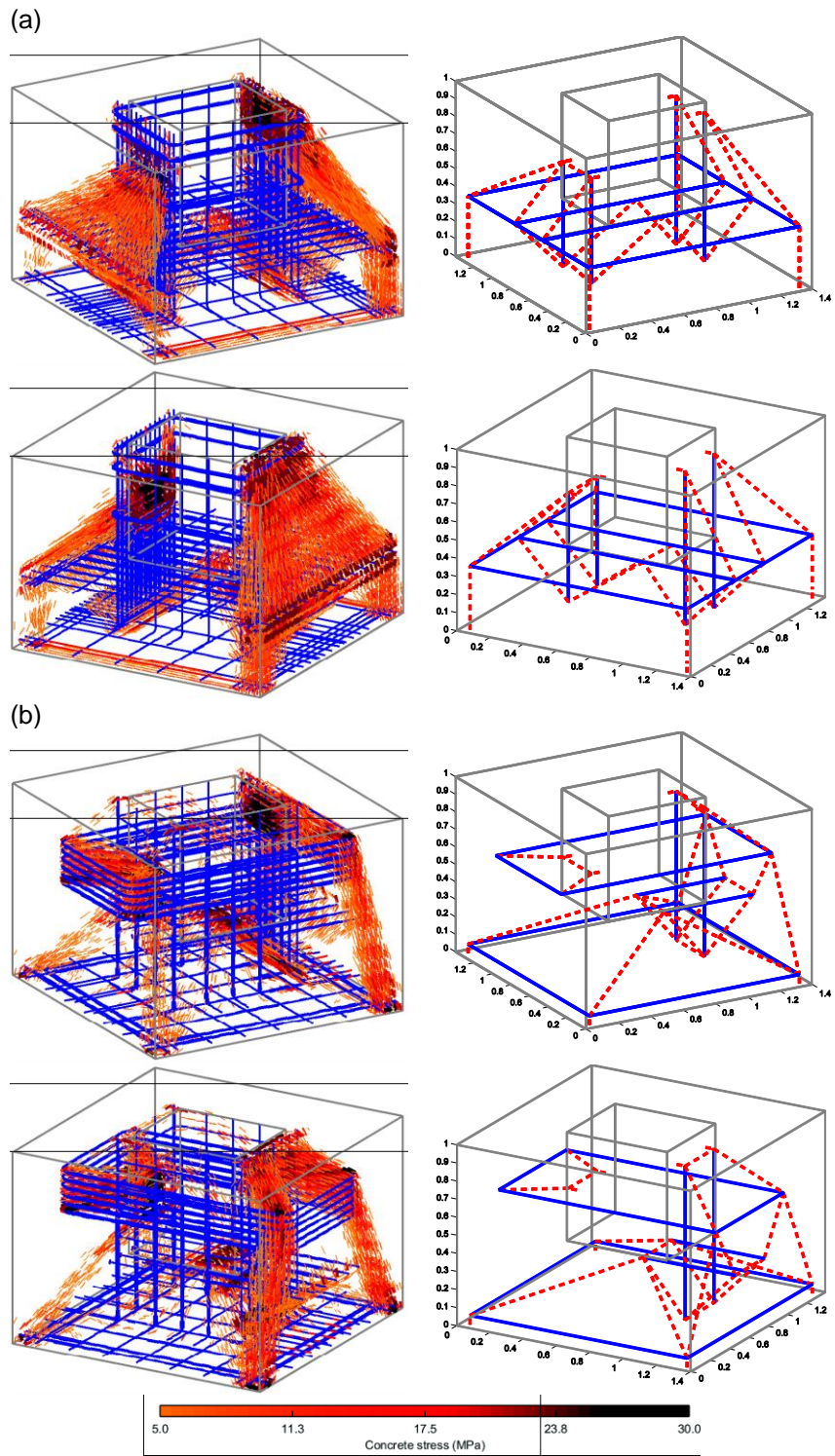


Figure 7. The FE model plot of the concrete principal compressive stress directions for specimen (a) X3 and (b) X7 ($FH=700kN$) (left) and the proposed strut-and-tie models (right).

Specimen	f_{cm} (MPa)	Rebars	$P_{max,exp}$ (kN)	Mode
BP-20-30-1 2	29.1 29.8	6-D10@120	485 480	B-S B-S
BPC-20-30-1 2	29.8 29.8	6-D10@40	500 495	B B
BP-30-30-1 2	27.3 28.5	8-D10@90	916 907	S B-S
BPC-30-30-1 2	28.9 30.9	8-D10@40	1039 1029	B-S B-S
BP-30-25-1 2	30.9 26.3	8-D10@90	794 725	B-S S
BPC-30-25-1 2	29.1 29.2	8-D10@40	853 872	B-S B-S

Table 1. Summary of the four-pile caps tested by Suzuki et al. [39]. *B: Flexural failure. S: Corner shear failure

Specimen	Souza et al. P^{STM} (kN)/SF	Elasto-plastic			Hognestad parabola			Mode ⁱⁱⁱ
		P^i (kN)/SF	P^{ii} (kN)/SF	P^{iii} (kN)/SF	P^i (kN)/SF	P^{ii} (kN)/SF	P^{iii} (kN)/SF	
BP-20-30-1	414/1.17	370/1.31	569/0.85	497/0.98	361/1.34	563/0.86	491/0.99	B-S
BP-20-30-2	414/1.16	371/1.29	580/0.83	494/0.97	355/1.35	565/0.85	497/0.97	B-S
BPC-20-30-1	414/1.21	446/1.12	631/0.79	499/1.00	440/1.14	618/0.81	507/0.99	B-S
BPC-20-30-2	414/1.20	446/1.11	631/0.78	499/0.99	440/1.13	618/0.80	507/0.98	B-S
BP-30-30-1	929/0.99	744/1.23	1098/0.83	866/1.06	723/1.27	1060/0.86	872/1.05	B-S
BP-30-30-2	929/0.98	748/1.21	1115/0.81	868/1.04	722/1.26	1086/0.84	857/1.06	B-S
BPC-30-30-1	929/1.12	933/1.11	1216/0.85	1004/1.03	898/1.16	1210/0.86	979/1.06	B-S
BPC-30-30-2	929/1.11	937/1.10	1235/0.83	983/1.05	890/1.16	1231/0.84	969/1.06	B-S
BP-30-25-1	929/0.85	617/1.29	1004/0.79	769/1.03	584/1.36	987/0.80	814/0.98	B-S
BP-30-25-2	929/0.78	575/1.26	937/0.77	742/0.98	586/1.24	904/0.80	737/0.98	S
BPC-30-25-1	929/0.92	747/1.14	1059/0.81	860/0.99	713/1.20	1027/0.83	860/0.99	B-S
BPC-30-25-2	929/0.94	748/1.17	1060/0.82	860/1.01	731/1.19	1028/0.85	861/1.01	B-S
μ (SF)	1.03	1.20	0.82	1.01	1.23	0.83	1.01	
CV (SF)	0.14	0.07	0.03	0.03	0.07	0.03	0.04	

Table 2. Predicted ultimate loads and the average μ and coefficient of variation CV of their corresponding safety factors SF. Notation: (i) neglecting concrete tensile strength; (ii) adopting the MCFT model; and (iii) adopting Hordijk's model. *B: Flexural failure. S: Corner shear failure